Environmental Science and Ecotechnology 31 (2026) 100708

Contents lists available at ScienceDirect

Environmental Science and Ecotechnology

journal homepage: www.journals.elsevier.com/environmental-science-and-ecotechnology/

Original Research

Trace lanthanum activation drives deep biological phosphorus removal

Bohan Liu [a], Jun Nan [a,*], Rongcheng He [a], Haiyang Wei [b], Tianyi Zhao [c], Yibo Zhang [a], Ruixue Jiang [a], Fangmin Wu [a], Zhencheng Ge [a], Xuesong Ye [a], Wei Wang [a,**], Jun Ma [a]

[a] State Key Laboratory of Urban-rural Water Resource & Environment, School of Environment, Harbin Institute of Technology, Harbin, 150090, China
[b] School of Civil Engineering and Transportation, Northeast Forestry University, Harbin, 150040, China
[c] School of Computer Science, Harbin Institute of Technology, Harbin, 150001, China

ARTICLE INFO

Article history:
Received 3 October 2025
Received in revised form
12 May 2026
Accepted 13 May 2026

Keywords:
Phosphorus removal
La-contained aerogel beads
Phosphate-accumulating organisms
La-enhanced biological phosphorus removal system
Wastewater treatment

ABSTRACT

Eutrophication driven by excessive phosphorus discharge threatens global aquatic ecosystems. Enhanced biological phosphorus removal (EBPR) is a sustainable, widely deployed wastewater treatment technology, yet it often requires optimization to meet increasingly stringent global phosphorus emission standards. Conventional chemical supplements can achieve deep phosphorus removal, but they require excessive dosing, generate large volumes of sludge, and can inhibit the essential polyphosphate-accumulating organisms (PAOs) that drive biological treatment. Here we show that a low-dose, slow-release lanthanum aerogel (LZGA) activates PAO metabolism, enabling deep biological phosphorus removal with a near-zero chemical footprint. By releasing La^{3+} into sequencing batch reactors, the LZGA platform reduced effluent total phosphorus from 0.85 mg L^{-1} to 0.14 mg L^{-1} at an optimal dose of 15 mg L^{-1}. This represents a two-order-of-magnitude reduction in chemical consumption compared to conventional precipitation methods, requiring 0.7 g of lanthanum to treat one ton of wastewater. Proteomic and microbial analyses reveal that trace La^{3+} stimulates potassium channels, upregulating key energy metabolism pathways and driving an order-of-magnitude increase in the protein expression of the core PAO *Candidatus* Accumulibacter. Furthermore, the system enhances extracellular polymeric substance (EPS) production, and improves the phosphorus absorption capacity of EPS. These findings demonstrate that targeted trace-metal activation of microbial metabolic pathways offers a strategy to upgrade existing bioreactors. This strategy provides a versatile paradigm for global wastewater management and advanced eutrophication control.

1. Introduction

Eutrophication of water bodies is a global environmental problem that threatens the sustainable development of human society [1]. Eutrophication can lead to harmful algal blooms, the death of biological organisms, disruption of local ecological equilibrium, and a decline in the quality of source water [2–4]. Eutrophication in surface water bodies is primarily attributed to the excessive input of phosphorus (P) from domestic and industrial wastewater [5,6]. Therefore, many countries have imposed strict limits on the effluent P concentrations from wastewater treatment plants (WWTPs). For example, the P standard for grade A domestic sewage effluent in China is less than 0.5 mg L^{-1}, and certain special areas must meet even stricter surface water standards of less than 0.3 mg L^{-1}. In the United States, specific regions—including Lake Tahoe, the Great Lakes, Occoquan Reservoir, Chesapeake Bay, and the Northern Gulf of Mexico—require even more stringent P emission standards of 0.1–0.2 mg L^{-1}.

Existing P removal technologies struggle to meet these increasingly stringent P emission requirements [7,8]. Enhanced biological phosphorus removal (EBPR) is among the most widely used technologies in over 70% of WWTPs worldwide due to its sustainability and low consumption [9,10]. Nevertheless, EBPR often faces challenges such as fluctuations in operating conditions,

* Corresponding author.
** Corresponding author.
E-mail addresses: nanjun119@163.com (J. Nan), wangweirs@hit.edu.cn (W. Wang).

https://doi.org/10.1016/j.ese.2026.100708

P-removal limitations, and modest biological activity, resulting in effluent total phosphorus (TP) concentrations of approximately 1.0 mg L^{-1}, which fail to meet relevant standards [11,12]. To address this issue, chemical P removal has been extensively applied in advanced treatment to further reduce P concentrations [13–15]. However, this method requires substantial amounts of chemical agents because excess doses are required to react with low concentrations of target pollutants [16]. Furthermore, the addition of chemical agents, such as polyaluminum chloride (PAC) flocculants, has a severe negative impact on polyphosphate-accumulating organisms (PAOs), reducing their proportion in the total bacterial population by over 50% and loosening *Zoogloea* structures. In turn, this reduces the activated sludge's capacity to combine with phosphate (PO_4^{3-}) by approximately 40% [17–20]. Additionally, the use of chemical agents generates large volumes of excess sludge, which significantly affects its subsequent treatment [21]. In summary, there is an urgent need to develop an effective, low-consumption P removal strategy that primarily relies on EBPR to reduce P concentrations to very low levels (e.g., below 0.2 mg L^{-1}) without the adverse side effects associated with chemical removal methods.

EBPR functions by capturing PO_4^{3-} through P uptake by PAOs during the aerobic stage [22–25]. Potassium ions (K^+) are generally metabolized concurrently with P in PAOs, serving as counterions to maintain cellular neutrality alongside the negatively charged polyphosphate [26,27]. Thus, activating K^+ channels in PAOs may be a key target for boosting P immobilization within these organisms. Discoveries in other bio-related areas can provide valuable ideas and inspiration. For instance, in cloned mammalian cells, low La^{3+} concentrations can interact with the negatively charged regions of K^+ channels via electrostatic interactions. This causes a moderate alteration in the protein structure of K^+ channels, thereby regulating their gating kinetics [28,29]. In the human body, trace amounts of La enhance the K^+-ATPase activity in human erythrocyte membranes [30]. Additionally, La modulates the expression levels of specific genes in hepatocytes and other cells [31–33]. Furthermore, at low La^{3+} concentrations, it can indirectly promote the transmembrane K^+ transport by altering the gating balance [34]. Given the high degree of structural and functional similarity between K^+ channels in bacteria and eukaryotes [35], we hypothesized that La^{3+} may also act on the K^+ channels of PAOs. By altering the gating equilibrium, La^{3+} may indirectly facilitate the transmembrane K^+ transport, thereby promoting the synergistic metabolism of K^+ and PO_4^{3-} and enhancing intracellular P accumulation.

Currently, most P-removal materials are in powder form. If La-based powdered materials are directly added to the EBPR system, although La^{3+} may be released, the materials are difficult to recover, leading to their continuous accumulation in the sludge. This can easily cause sludge deterioration, reduced microbial activity, and deterioration of the effluent quality. Moreover, nano-sized powders tend to agglomerate, which can significantly reduce their chemical P-capture capacity and bioavailability. Meanwhile, the release of La^{3+} from the powdered materials is uncontrollable, leading to excessively high local La^{3+} concentrations and thereby inhibiting microorganism activity. Therefore, this study proposed loading lanthanum hydroxide ($La(OH)_3$) into millimeter-scale aerogel beads with a multilevel pore structure, and by controlling the release, to achieve a continuous and low-dose supply of La^{3+}, while ensuring the recyclability and stability of the material.

In this study, we developed a La activation-based strategy to enhance biological P removal in wastewater treatment. La-containing aerogel beads (LZGA) were specifically designed and used as a source of La to bolster the performance of sequencing batch reactors (SBR). LZGA has a highly selective P-removal capacity and strong anti-interference ability, making it useful for sewage treatment. As a La library, LZGA can also release La^{3+} slowly and enhance the biological P removal capability. Based on the aforementioned description, this study proposed a new strategy for La-enhanced P removal, aiming to achieve efficient, low-consumption deep P removal by precisely targeting and regulating PAO activity with a small amount of La^{3+}. The long-term stability of LZGA in the EBPR system was evaluated by conducting a detailed study on the changes in P removal efficiency in the SBR. Using 16S rRNA and proteomics analyses, we identified changes in microbial community structure and key protein pathways in the La-EBPR system, providing a molecular-level explanation for the biochemical cooperative P-removal mechanism of LZGA. This development proposes a novel and efficient strategy to enhance P removal for wastewater treatment.

2. Materials and methods

2.1. Loading La components into microcapsules

We synthesized LZGA beads through an *in situ* crosslinking interaction method. First, graphene oxide (GO) was added to 100 mL of distilled water, and the samples were ultrasonicated for 15 min to ensure complete dispersion of GO in the deionized water, forming a GO dispersion liquid stock at a concentration of 3 g L^{-1}. Afterward, 2 g of sodium alginate (SA) and 6 g of $La(OH)_3$ were each added to 50 mL of distilled water. These three solutions were then mechanically stirred at room temperature for 24 h to obtain a uniform mixture. The resulting mixed solution was injected into a 1000 mL cross-linking solution containing 1% ethanol and 3% zirconium oxychloride ($ZrOCl_2{\cdot}8H_2O$) (w/v) using a 10 mL syringe. The spherical hydrogel beads formed in the cross-linked solution were soaked for 24 h to ensure complete cross-linking reactions. Then, the hydrogel beads were washed 3–5 times with distilled water to eliminate any unreacted metal ions. Lastly, the hydrogels were freeze-dried for 24 h to produce the LZGA material. All chemicals used in this study were of high purity and met analytical reagent standards (further details are provided in the Supplementary Information).

2.2. Reactor set-up and operational conditions

In this study, we constructed plexiglass SBRs equipped with mechanical agitators, as depicted in Supplementary Fig. S1. The SBRs were operated in four 6-h cycles per day. At the start of each cycle, 1 L of untreated raw sewage was introduced, and 1 L of treated effluent was discharged at the end of the cycle. Each cycle comprised 5 min of influent, 85 min of anoxic reaction, 210 min of aerobic reaction, 45 min of settling, and 15 min of effluent discharge. During both the anoxic and aerobic phases, the mechanical agitator was operated at 150 rpm. In the aerobic stage, air was supplied to the SBRs to maintain a dissolved oxygen concentration of approximately 4.0 mg L^{-1} using aeration diffusers powered by electromagnetic air compressors. The reactors were inoculated with activated sludge obtained from the Taiping Wastewater Treatment Plant (Harbin, China), and the initial mixed liquor suspended solid concentration in the reactors was approximately 3500 mg L^{-1}. The sludge retention time was set at 18 d. The inlet water of the reactors was municipal conventional domestic sewage, with influent chemical oxygen demand (COD), total nitrogen (TN), and TP concentrations of approximately 400, 20, and 5 mg L^{-1}, respectively. LZGA beads were loaded into a Teflon mesh (1 mm × 2 mm), which facilitated their separation from the mud-water mixture. These loaded beads were then introduced into the

SBRs during the aerobic phase of the reaction. The LZGA beads were easily removed from the Teflon cage and reactivated for reuse. The entire operation was conducted in a temperature-controlled room maintained at 25 °C.

2.3. Analytical methods

The surface morphologies of both LZGA and activated sludge were examined using a 3D measuring laser microscope (OLS5000, Olympus Corporation, Tokyo, Japan), a digital microscope (DSX1000, Olympus Corporation, Tokyo, Japan), and a HeliosNanolab600i (FEI Company, Hillsboro, Oregon, USA) field emission scanning electron microscope (FE-SEM). Fourier-transform infrared spectroscopy (FT-IR) was used to analyze the functional groups in LZGA before and after P capture, with potassium bromide as the reference. The LZGA structural characteristics were assessed using X-ray diffraction (XRD). Moreover, X-ray photoelectron spectroscopy was conducted to investigate the binding energy of elements before and after P capture. Thermal analysis data (TGA) were obtained using a STA449C instrument (NETZSCH, Bayern, Germany) from room temperature to 800 °C at a heating rate of 10 °C min^{-1} under a nitrogen atmosphere. The presence of dissolved La ions in water was detected using inductively coupled plasma-optical emission spectrometry (ICP-OES).

In this study, we analyzed conventional wastewater pollutants such as COD, NH_4^+-N, TN, and TP, as well as activated sludge characteristics, according to standard procedures [36]. Extracellular polymeric substances (EPS) were analyzed for protein and polysaccharide (PS) concentrations and extracted from the sludge mixture by thermal treatment [37]. The protein concentration was determined using a modified version of the Lowry procedure [38], whereas the PS content was determined through a sulfuric acid-anthrone colorimetry method [39].

2.4. Microbial community analysis

We investigated the microbial community composition within the activated sludge system incorporating LZGA using high-throughput sequencing. Six samples were collected after 80 days of operation, with LZGA aerogel bead concentrations of 0, 5, 10, 15, 20, and 30 mg L^{-1}. Genomic DNA from the microbial community was extracted from the activated sludge using the E.Z.N.A.® soil DNA kit (Omega Bio-tek, Norcross, GA, USA) according to the manufacturer's instructions. The quality and quantity of the DNA extracted were assessed using both a 1% agarose gel and a NanoDrop 2000 UV-vis spectrophotometer (Thermo Scientific, Wilmington, USA). The 16S rRNA gene (V3-V4 region) was amplified using the 341F (5′-CCTACGGGNGGCWGCAG-3′) and 805R (5′-GACTACHVGGGTATCTAATCC-3′) primer pair with an Applied Biosystems GeneAmp® 9700 PCR thermocycler (Applied Biosystems, Foster City, CA, USA). Sequence analysis was conducted as described by Gao et al. [40].

2.5. Proteomics

Sludge samples with LZGA aerogel bead concentrations of 0 (control) and 15 mg L^{-1} were collected on day 80. Protein identification was conducted in triplicate. Protein concentrations were determined using the BCA Protein Assay kit (Beyotime Biotechnology, Shanghai, China). Protein digestion was conducted following standard procedures [41]. Enzymolysis and LC-MS/MS protein analysis were then performed. The original MS/MS spectra files were imported into the ProteomeDiscoverer™ software (version 2.4) for analysis. The false discovery rate for peptide identification was $\leq$0.01, and the identified protein contained at least one specific peptide. The protein abundance data obtained from the database were subjected to statistical analysis to identify differentially expressed proteins (DEPs). *P* values were calculated using a Student's *t*-test ($P < 0.05$), and proteins with a fold change of more than 1.2 times were identified as DEPs. Annotation of all identified proteins was conducted using Gene Ontology (http://geneontology.org/) and the Kyoto Encyclopedia of Genes and Genomes (KEGG) pathway (http://www.genome.jp/kegg/). DEPs were further subjected to Gene Ontology and KEGG enrichment analysis.

3. Results and discussion

3.1. Loading La components into aerogel beads and LZGA characterization

To address the challenges of recycling powdered materials from wastewater, which can lead to excessive La accumulation, changes in microbial community structure over prolonged operation, and the wastage of water treatment agents, we devised a strategy that incorporated La into aerogel beads featuring a macro-micro-multistage structure. Briefly, we mixed commercial powdered $La(OH)_3$ (Supplementary Fig. S2) with SA and GO in water. Then, the mixture was injected into a cross-linked solution containing ethanol and $ZrOCl_2$ to form spherical hydrogel beads. After freeze-drying, we obtained La-embedded LZGA where $La(OH)_3$ acted as the functional component, Zr(IV) and SA served as the skeletons through a crosslinking reaction between cations and carboxyl groups, and GO provided mechanical reinforcement (Fig. 1a). As illustrated by the laser scanning confocal microscopy (LSCM) image (Fig. 1b) and the optical photograph in Supplementary Fig. S3, the LZGA prepared exhibited uniform spherical particles with an average diameter of approximately 3 mm. Upon examining a cross-section (Fig. 1c), the beads exhibited a unique honeycomb mesh structure with an aperture of approximately 200 μm (Fig. 1d), likely due to van der Waals forces and π-π stacking effects associated with the GO layer [42]. This highly porous structure facilitated the mass transfer of wastewater inflow and the delivery of La components into the wastewater. The LZGA surface morphology was characterized at multiple scales using LSCM and FE-SEM. The LSCM image (Fig. 1b) shows that the microsphere surface exhibited pronounced non-uniform textures and undulations. To further analyze the microstructure, the FE-SEM image (Fig. 1e) showed a wrinkled surface, consistent with the macroscopic features observed by LSCM. Additionally, most traditional hydrogel beads without GO would shatter after freeze-drying. In contrast, with the addition of GO, the LZGA mechanical properties were significantly improved, and after freeze-drying, the LZGA remained intact and did not break apart. The XRD patterns of the LZGA beads (Fig. 1f) confirmed their crystalline structure. The diffraction peaks in the XRD spectrum is attributed to the $La(OH)_3$ crystal phase (JCPDS No. 36-1481) [(100), (110), (101), (200), (111), (201), (210), (002), (300), (211), (102), (112), (220), (202), (310), (311), (212), (400), (302)], indicating that $La(OH)_3$ was successfully loaded onto the SA-GO framework and maintained the hexagonal crystal structure. The LZGA chemical composition was also characterized through TGA (Supplementary Fig. S4) and ICP-OES. The loading ratio of La in the LZGA was approximately 4.62%.

3.2. Boost of biological P removal in sewage

The LZGA prepared was used as the source of La to enhance sewage treatment in SBRs. We used six SBRs, each containing activated sludge, which provided a necessary environment for

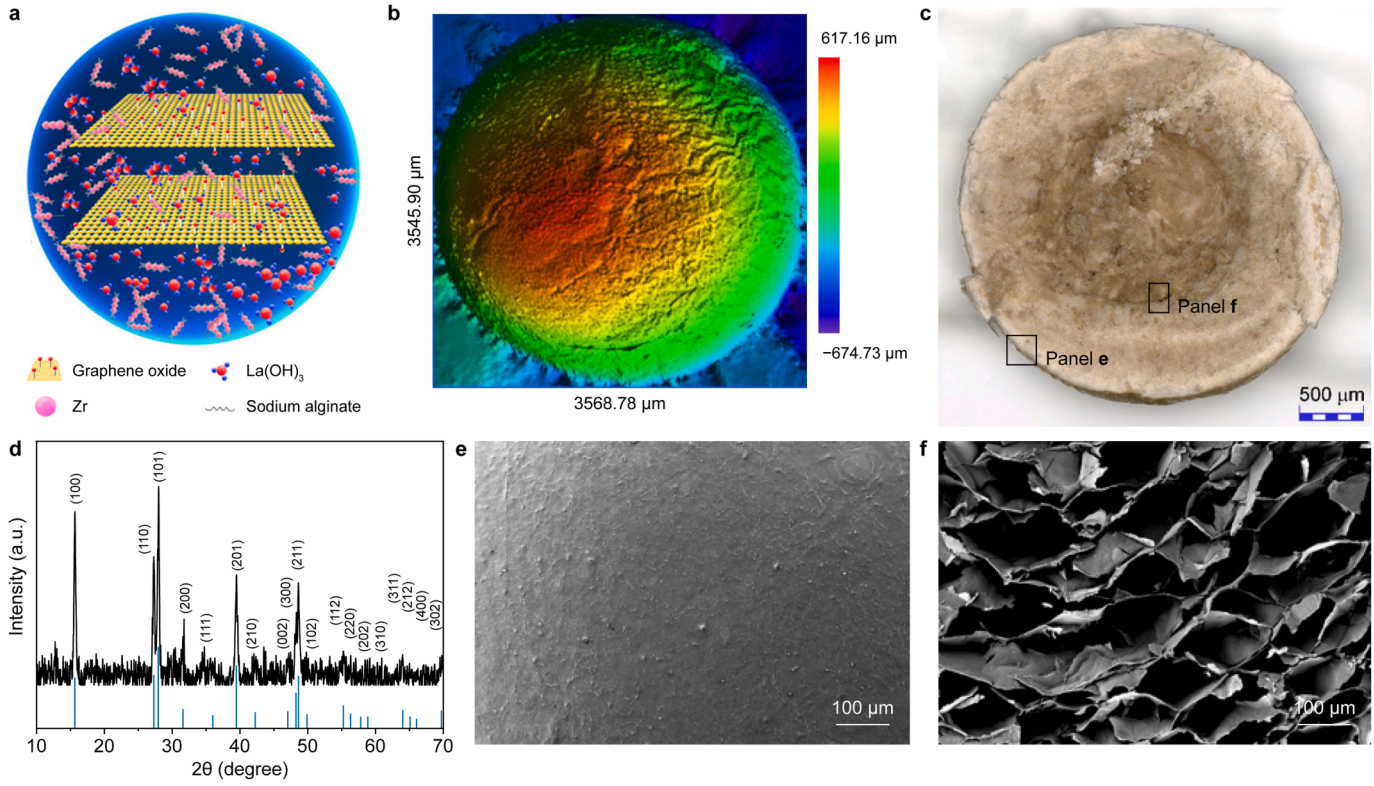

Fig. 1. Characterization of La-containing aerogel (LZGA). **a**, Schematic illustration of the LZGA structure. **b**, Three-dimensional laser scanning confocal microscopy topography of LZGA surface. **c**, Optical micrograph of LZGA cross-section. **d**, X-ray diffraction pattern of LZGA. **e**–**f**, Scanning electron microscopy images of the LZGA surface (**e**) and cross-section (**f**).

microorganisms to thrive. Each SBR was used to treat 4 L of sewage water daily. In the initial 20 days, no LZGA was added (Phase I). During this period, 16S rRNA analysis was used to assess the stability of the microbial community in the activated sludge. All six SBRs reached steady state, with the average effluent COD and TN concentrations meeting the standards for grade A effluent from domestic sewage in China. However, the effluent TP concentrations from the six traditional SBRs remained at approximately 1.0 mg L^{-1} (Supplementary Fig. S5). Starting from day 21 (Phase II), six different LZGA bead concentrations (0, 5, 10, 15, 20, and 30 mg L^{-1}) were added to the SBRs over the following 60 days to establish La-EBPR systems. Compared to the control group (traditional SBR without LZGA), the experimental group exhibited a significant decrease in the effluent TP concentration (Fig. 2a). When 15 mg L^{-1} of LZGA was introduced to the activated sludge SBR system, the average TP concentration consistently decreased to a very low value of 0.19 mg L^{-1}. Furthermore, from day 60 onward, the TP concentration in this system reached an exceptionally low level of 0.14 mg L^{-1}, indicating long-term stability and high efficiency. The La-EBPR systems reduced effluent TP by approximately 6-fold compared to traditional EBPR (0.85 mg L^{-1}). The effect of the LZGA dosage on P removal performance was also investigated (Fig. 2b). The removal efficiency increased with increasing dose, but the effluent TP concentration decreased only slightly when the dose exceeded 15 mg L^{-1}. Therefore, we concluded that the optimal LZGA dose in this system was 15 mg L^{-1}.

To identify the role of LZGA in activating EBPR, we designed additional control experiments. The TP concentration was set at 0.85 mg L^{-1}, which matches the effluent TP concentration of traditional EBPR before the introduction of LZGA. When 15 mg L^{-1} of LZGA beads were introduced into the PO_4^{3-} solution without activated sludge, the remaining P concentration was 0.67 mg L^{-1} (Fig. 2c), resulting in a low removal efficiency of only 21.1%. In contrast, after adding 15 mg L^{-1} LZGA into the SBR, which contained activated sludge and consequently, PAOs, the effluent TP concentration was reduced to 0.14 mg L^{-1} in the La-EBPR system. This indicates that although LZGA has La reactive sites for chemically capturing P (Supplementary Fig. S6), this low LZGA dose alone cannot effectively reduce P to a significantly low level. The P capture by LZGA itself accounted for only approximately 25% (chemical capture), whereas most of the P removal efficiency (75%) was attributed to EBPR enhancement facilitated by the LZGA leveraging function. Furthermore, to verify whether substances in LZGA other than La influenced PO_4^{3-} removal, we also examined the effect of unloaded $La(OH)_3$ aerogel beads on the activated sludge system. Our findings confirmed that these unloaded beads did not significantly contribute to P removal (Supplementary Fig. S7). Therefore, based on these comparative experiments, we concluded that La is a functional component of LZGA and significantly enhances P removal in the activated sludge system.

To emphasize the advantages of the La-EBPR system, we compared its P removal performance with that of several conventional chemical removal technologies (Fig. 2d). The most used technology is coagulation with PAC or ferric salts as coagulants. However, PAC concentrations above 300 mg L^{-1} are typically required to reduce the effluent P concentration to less than 0.20 mg L^{-1}, even when combined with polyacrylamide [43,44]. Ferric salts are unable to reduce the effluent P concentration to nearly 0.10 mg L^{-1} in wastewater treatment [45]. In addition to the coagulation technology, adsorption is another promising chemical method for P removal. However, it required substantial amounts of

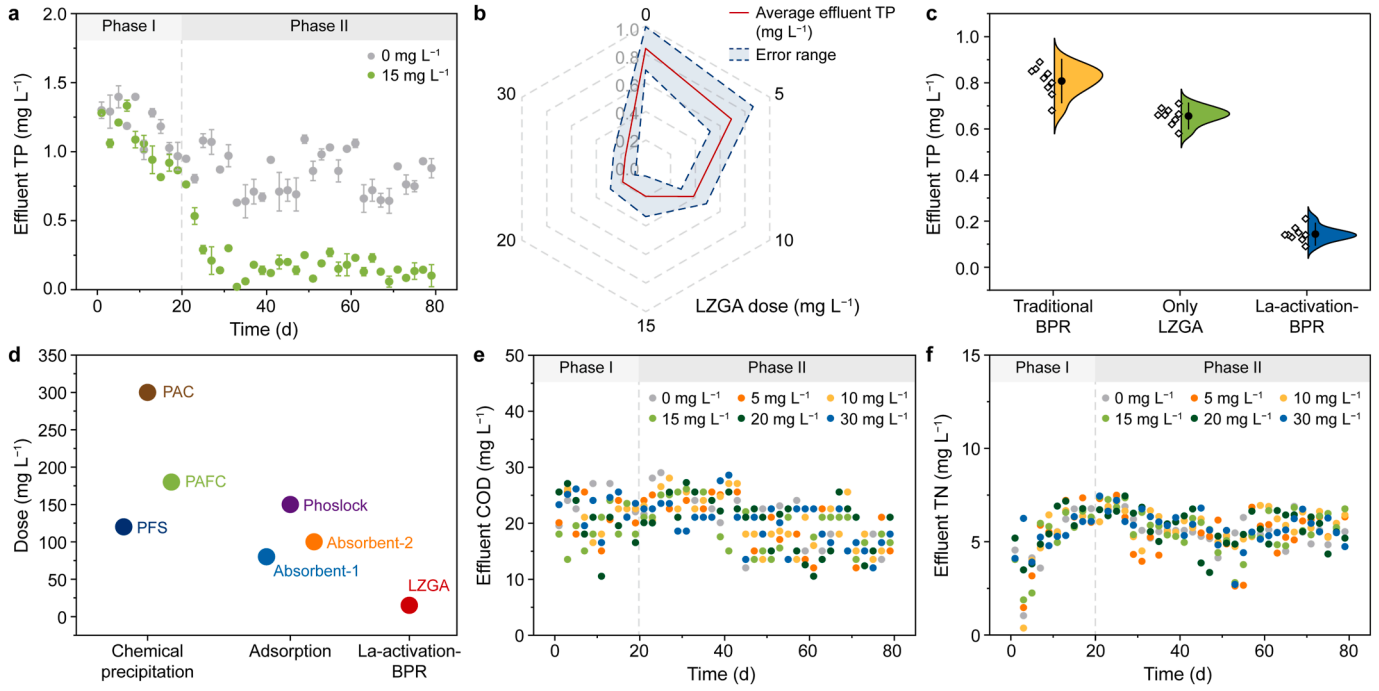

Fig. 2. Effluent performance of the lanthanum-enhanced biological phosphorus removal (La-EBPR) system. a, Time-dependent variation in effluent total phosphorus (TP) in traditional EBPR and La-EBPR systems amended with 15 mg L^{-1} La-containing aerogel (LZGA). Error bars represent the standard deviation of *n* independent measurements ($n = 3$). **b**, Average effluent TP at different LZGA concentrations. Error bars represent the standard deviation of *n* independent measurements ($n = 3$), and the red data line shows the mean. **c**, Effluent TP in different methods. Error bars represent the standard deviation of *n* independent measurements ($n = 3$), and the circular data points represent the mean. Scatter represents independent measurement samples. **d**, Comparison of chemical addition levels in the La-EBPR system and other methods. **e**–**f**, Time-dependent variation in effluent chemical oxygen demand (COD, **e**) and total nitrogen (TN, **f**) at different LZGA concentrations.

adsorbents (Fig. 2d), often tens or even hundreds of grams of La-containing components, to reduce P to 0.1–0.2 mg L^{-1} [46–48]. In the La-EBPR system, with the La content of functional components in LZGA at 46.2 mg g^{-1}, only 0.7 g of La was required to purify 1 ton of wastewater, reducing the TP concentration from 0.85 to 0.14 mg L^{-1}. In other words, the La-EBPR system can achieve a nearly two-order-of-magnitude reduction in chemical consumption compared to traditional chemical precipitation and adsorption methods. In addition to studying P removal, we investigated other typical water treatment parameters in the La-EBPR system. In this study, we observed that LZGA had no significant impact on the removal of other nutrients (Fig. 2e and f). Therefore, the introduction of LZGA specifically enhanced the removal of PO_4^{3-} in the La-EBPR system without exerting a noticeable effect on other nutrients.

3.3. Activation of P access

Our findings demonstrated that the active La components migrated outward slowly and continuously from the LZGA beads. The La^{3+} release capacity remained nearly constant at approximately 18 mg g^{-1} in solutions with a pH range of 6–8 (Supplementary Fig. S8). However, as the pH increased to 9, the La^{3+} release capacity decreased significantly, reaching only 13 mg g^{-1} within 24 h. This can be attributed to the fact that most of the $La(OH)_3$ embedded in LZGA was activated by the slightly acidic environment of the $ZrOCl_2$ cross-linked solution, and the activated La formed dynamic coordination bonds with the -OH of the alginate ligand. Under acidic or neutral conditions, the active La components were more prone to migrate slowly and sustainably outward in an ionic state. At pH 6, the La^{3+} release rate from LZGA was the highest during the first hour (12.08 mg g^{-1}) and gradually decreased thereafter. After 24 h, no further La^{3+} release was observed, with a total release of 18.4 mg g^{-1}. Additionally, the La component content before and after release was analyzed, revealing that 27.3 mg g^{-1} of La remained in the LZGA after release. Following activation of the La components, most of the remaining La continued to be released (Supplementary Table S1). Furthermore, no other metal ions were released from LZGA except for La^{3+}. Based on the slow-release effect of La components, we hypothesized that the continuous release of the active La components from LZGA may enhance PO_4^{3-}removal by certain microorganisms, leading to reduced P concentration.

To test this hypothesis, changes in the activated sludge in the La-EBPR system were studied. After 80 days of inoculation in the reactors, the activated sludge system was mainly composed of cocci and bacilli, with a small number of filamentous bacteria (Supplementary Fig. S9). Compared to the control reactor, the treated sludge exhibited a plump, dense, and block-like structure, indicating that the introduction of 15 mg L^{-1} LZGA improved the morphology of the sludge (Fig. 3a). Additionally, similar results were obtained in the sludge particle size distribution diagram (Supplementary Fig. S10).

EPSs are crucial components that affect the physicochemical and biological properties in biological flocculation. Previous studies have shown that EPS can promote biological flocculation [49–51]. For example, EPS contains hydrophobic molecules, such as lipids and proteins, that can render the sludge surface partially hydrophobic and enhance flocculation. The changes in EPS varied across different LZGA concentrations (Fig. 3b). PS in EPS showed no significant differences among the SBRs, suggesting that LZGA was not directly correlated with PS. In contrast, protein concentration exhibited more pronounced changes. Compared to the control group, when the LZGA concentrations ranged between 5 and

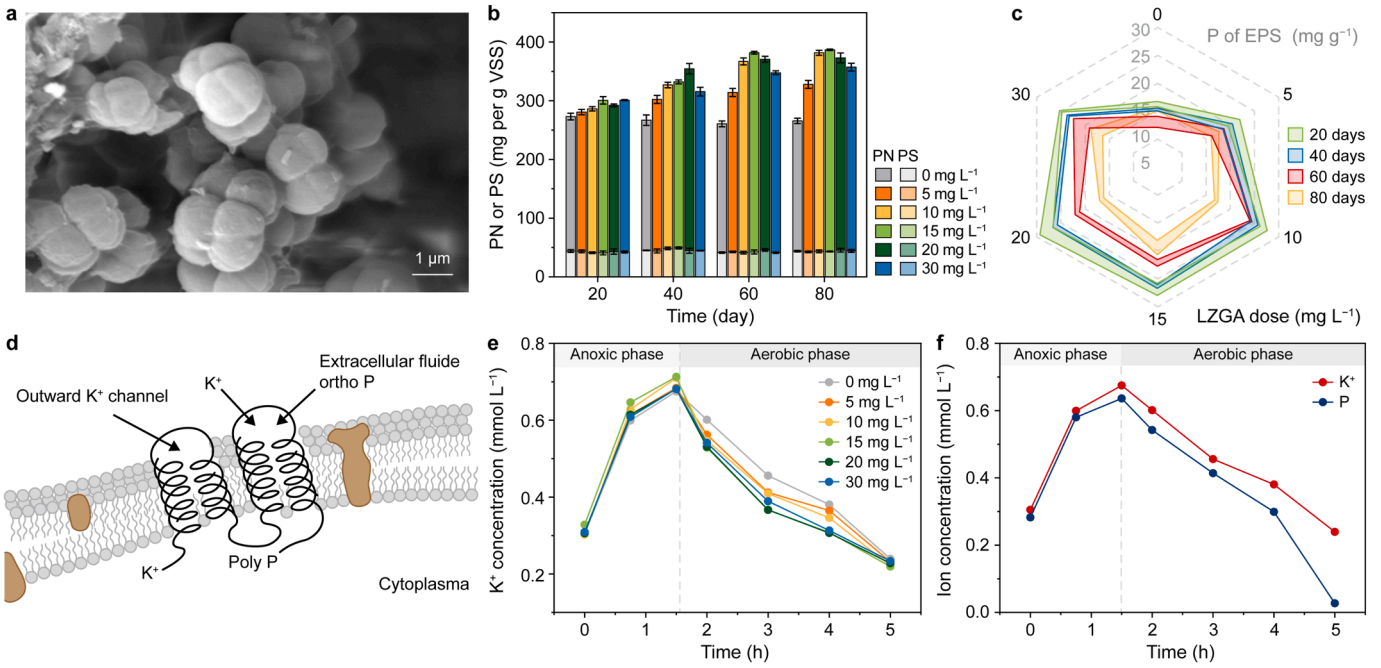

Fig. 3. Activation of phosphorus uptake in the lanthanum-enhanced biological phosphorus removal (La-EBPR) system. a, Scanning electron microscopy image of sludge from the La-EBPR system amended with 15 mg L^{-1} La-containing aerogel (LZGA). **b**, Effects of LZGA concentrations on the production of protein (PN) and polysaccharide (PS) in extracellular polymeric substances. Error bars represent the standard deviation of *n* independent measurements ($n = 3$). **c**, Changes in EPS-associated phosphorus concentration in reactors operated at different LZGA doses. **d**, Schematic diagram of the outward K^+ channel associated with phosphorus transport. **e**, Effects of LZGA concentrations on K^+ concentration over the operational cycle. **f**, Synchronous metabolism in K^+ and phosphorus concentrations during the cycle.

10 mg L^{-1}, the protein concentration increased steadily from 237.0 ± 4.5 to 285.3 ± 6.8 and 245.1 ± 3.8 to 338.1 ± 4.3 mg per g MLVSS (mixed liquor volatile suspended solids) over 60 d, respectively. When LZGA doses were between 15 and 30 mg L^{-1}, the protein content reached its maximum at day 60 and remained relatively stable for the next 20 d. Therefore, we concluded that the protein concentration reached a stable state at 40 days with LZGA doses higher than 15 mg L^{-1}. Notably, the most significant increase in protein concentration occurred when 15 mg L^{-1} LZGA was added to the reactors, rising from 259.9 ± 6.4 to 363.6 ± 1.2 mg per g MLVSS. After that, the increase in protein concentration decreased slightly with the increasing dose but remained higher than that of the control group. Thus, the higher LZGA addition does not necessarily increase EPS. In fact, excessive LZGA may inhibit the production of some proteins in EPS, thus reducing the overall EPS content. Proteins in EPS can enhance the stability of sludge flocs and their resistance to external toxins due to its hydrophobic nature [52–55]. Therefore, the increased EPS, especially proteins, at appropriate LZGA concentrations likely contributes to stability in biological flocculation, which aligns with the observed increase in sludge particle size. Increased EPS might not be conducive to the flocculation and sedimentation of activated sludge due to the negatively charged functional groups in EPS, which could lead to sludge bulking and reduced microorganism ability to remove pollutants [56,57]. However, in this La-EBPR system, despite the increased EPS content, the sludge sedimentation performance did not deteriorate. In fact, it improved by 35%, 24%, 21%, 24%, 18%, and 23% after 80 days of activated sludge cultivation in the SBRs. This demonstrates that LZGA promoted the release of active La components, which then combined with the floc surface to neutralize the negative charge on the sludge surface, thereby improving sludge sedimentation performance. Therefore, our findings indicate that the addition of LZGA not only increased EPS production but also improved sludge flocculation and sedimentation performance.

The EBPR process traditionally focuses on enriching PAOs by alternating anaerobic and aerobic conditions. PAOs play a crucial role in removing P from wastewater by metabolizing polyphosphate [22–25]. However, studies have suggested that EPS also contributes to P removal. For example, Cloete et al. reported that EPS contains 27–30% P and could be considered a dynamic reservoir for P in sludge flocs [58]. Li et al. also found that EPS participates in the EBPR process and plays an important role in the P removal system [59]. The addition of LZGA induced changes in the phosphorus content of EPS (Fig. 3c). Our findings demonstrate that P contents in EPS increased significantly with the addition of the beads. By day 80, 15 mg L^{-1} LZGA promoted the EPS matrix around PAOs to capture P, resulting in an increase in P contents from 19.4 ± 1.3 to 26.9 ± 1.1 mg g^{-1}, which was 10.6 mg g^{-1} higher than that of the control group. The protein and PS in EPS are both polymers capable of bridging pollutants and adsorbing multiple colloidal particles via ionic, hydrogen, and van der Waals forces. The active La components released from LZGA can enhance the bridging effect of EPS. In particular, La^{3+} can link proteins and PS on the cell surface of microorganisms, reducing electrostatic interactions between polymers and pollutants and thereby strengthening P capture. Therefore, the addition of LZGA can not only increase the amount of EPS but also enhance the capture of P in EPS.

Additionally, P is an important element for maintaining the life processes of a cell. Ion channels are crucial components of cell membranes, forming the most sensitive system to foreign substances. K^+ channels are the most widely distributed ion channels [34] (Fig. 3d). When the membrane potential changes, K^+ channel proteins receive electrical stimulation, resulting in changes in molecular configuration and the functional state of the channel (i.e., the opening and closing of the channel). In this study, LZGA released La^{3+} continuously and slowly. The surface of K^+ channel

proteins contains regions with a concentration of negative charges that serve as binding sites for La^{3+}. When a low La^{3+} concentration was captured on the cell membrane, a large number of stable complexes were not easily formed. La^{3+} moderately interfered with K^+ channel proteins, mainly through noncovalent coordination, thereby accelerating K^+ channel switching [28,29]. This aligns with our experimental conclusion. La^{3+} released from LZGA accelerated K+ channel switching, and the K^+ concentration in the La-EBPR system environment was significantly lower than that in the control group during the aerobic phase (Fig. 3e), suggesting that more K^+ entered the cell. Notably, K^+ always acted as a polyphosphate counterion to maintain cell neutrality [26,27]. In the EBPR system, K^+ and PO_4^{3-} were released and absorbed simultaneously (Fig. 3f). Therefore, the slow release of La^{3+} from LZGA improved the K^+ channels of the cell membrane, effectively enhancing the synchronous metabolism of K^+ and P.

3.4. Effect of LZGA on the microbial community structure

To further determine the effect of LZGA on microorganisms, especially PAOs, we conducted 16S rRNA analysis to assess microbial community diversity in the activated sludge. Significant differences in operational taxonomic units were observed after adding LZGA to the reactors (Table 1), indicating that the beads had a significant impact on microbial diversity and richness in the activated sludge system. Species richness was evaluated using Chao1 and the abundance-based coverage estimator (ACE), whereas species diversity was assessed using the Shannon and Simpson indices, as previously described [60]. Compared with the control group, both the ACE and Chao1 indices increased significantly in all reactors with LZGA, suggesting that the beads promoted microbial community species richness in the activated sludge system. Regarding the Shannon indices, microbial diversity in the SBRs initially increased, then slightly decreased as LZGA doses increased. These results indicated that lower levels of LZGA beads increased species richness and microbial diversity. However, with the continuous release of La, the ecosystem selectively favored species better suited to survive under the prevailing conditions, resulting in greater specificity in the sludge.

To investigate changes in the microbial community within the La-EBPR system, we examined the relative abundances at different taxonomic levels (results at the phylum and class levels are shown in Supplementary Fig. S11). At the genus level, the dominant bacterial groups were identified as *Acinetobacter* (Fig. 4), which has been recognized as the dominant microbial species involved in P removal in EBPR [61,62]. The proportion of *Acinetobacter* increased from 12.2% to 15.9% after the addition of LZGA. Additionally, *Dechloromonas* and *Hydrogenophaga* were reported as denitrifying polyphosphate-accumulating organisms (DPAOs) capable of denitrifying and removing PO_4^{3-} simultaneously [62]. The proportions of *Dechloromonas* and *Hydrogenophaga* increased from 0.9% to 2.9% and from 0.1% to 1.0%, respectively, with the addition of 15 mg L−1 LZGA, and then decreased at higher doses. Similarly,

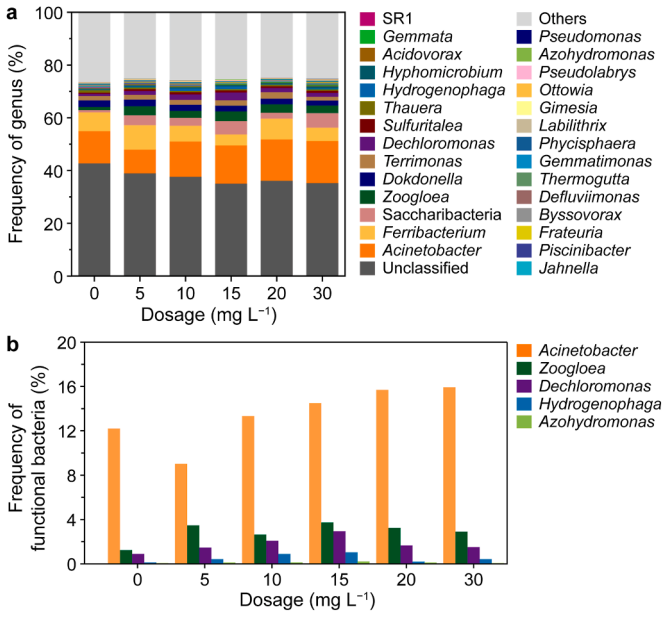

Fig. 4. Effect of La-containing aerogel (LZGA) on microbial community structure. **a**, Genus-level bacterial community structures in the traditional enhanced biological phosphorus removal (EBPR) and La-EBPR systems. **b**, Relative abundances of functional bacteria in the traditional EBPR and La-EBPR systems. Abundances are expressed as percentages of the total effective bacterial sequences in the sludge samples.

the relative abundance of *Azohydromonas* initially increased and then decreased as LZGA concentrations increased, reaching a maximum of 0.2% with the addition of 15 mg L^{-1} LZGA. Although *Azohydromonas* has not been proven to be a typical PAO, it significantly affects the degradation of organophosphorus pesticides [63]. In contrast, *Zoogloea* are not only members of the DPAOs but are also essential for EPS formation in activated sludge [64]. Their abundance increased from 1.2% in the control group to 3.7% with the addition of 15 mg L^{-1} LZGA, and then decreased to 2.9%. These results were consistent with the previous analysis of EPS, indicating that an appropriate La concentration promoted EPS formation. Therefore, appropriate LZGA concentrations increased the contents of PAOs (including DPAOs) and EPS in the activated sludge system, thereby promoting P removal.

Although 16S rRNA analysis offers high-throughput advantages for analyzing microbial community structure, it has limitations in accurately identifying and quantifying specific microbial groups with complex metabolic functions. For instance, *Candidatus* Accumulibacter is a key member of the PAO group. Due to the high conservation of the 16S rRNA gene sequence and the similarity to closely related species, it might have been underestimated in this analysis [10]. Therefore, 16S rRNA analysis primarily revealed the trend in LZGA's effect on the microbial community's overall structure. To more directly and precisely reveal the activating

Table 1
Effect of LZGA on the microbial richness and diversity of activated sludge.

LZGA concentration (mg L^{-1})	OTU number	Shannon index	ACE index	Chao1 index	Simpson index
0	1710	5.37	2291.81	2184.77	0.02
5	1708	5.49	2489.76	2470.53	0.02
10	1912	5.48	2662.03	2600.02	0.02
15	1745	5.42	2495.83	2400.00	0.02
20	1749	5.10	2493.17	2392.77	0.03
30	1966	5.42	2643.28	2532.34	0.03

LZGA, La-containing aerogel. OTU, operational taxonomic unit. ACE, abundance-based coverage estimator. The 0 mg L^{-1} treatment served as the control.

effect of La on the P-removal function of PAOs, it is necessary to use analytical methods that reflect the actual physiological state of microorganisms and the expression of functional proteins.

3.5. Proteomics and the response mechanism of the La-EBPR system

To overcome the limitations of 16S rRNA sequencing for functional analysis and to directly investigate the molecular-level impact of LZGA on PAO activity, we conducted macro-proteomics analysis of sludge samples from the control and optimal treatment groups (15 mg L^{-1} LZGA). This method can directly detect the expression abundance of functional proteins in the microbial community, thereby accurately identifying the changes in the PAO functional protein pathways in the La-EBPR system. We consistently identified 4657 proteins across three replicates. The changes in protein species and expression levels were most pronounced 20 days after the addition of 15 mg L^{-1} LZGA, and 1642 proteins exhibited a significant abundance change (Fig. 5a–d). As LZGA continued to be added over time, these changes gradually decreased. After 60 days, the protein composition and content remained relatively stable compared with 20 days earlier, indicating that the La-EBPR system had reached a steady state, consistent with previous findings. The protein expression level of *Candidatus* Accumulibacter exhibited the most significant change following LZGA addition, increasing by an order of magnitude from 7.9×10^8 to 2.6×10^9. *Candidatus* Accumulibacter is widely recognized as one of the most representative PAOs in sewage treatment [62], suggesting that LZGA promotes PAO growth and enhances protein expression, thereby facilitating PAO-mediated P removal. Furthermore, all proteins exhibiting significant changes in expression were subjected to unsupervised clustering and were grouped according to the similarity of their responses to different treatments The classification of DEPS on Gene Ontology revealed a significantly higher abundance of proteins related to metabolic processes, cellular processes, cellular anatomical entities, catalytic activity, and binding in the La-EBPR system compared to the control group (Fig. 5e). In contrast, enrichment analyses of the DEPs-based on Clusters of Orthologous Groups provided more intuitive explanations, showing that proteins related to inorganic ion transport and metabolism, lipid transport and metabolism, amino acid transport and metabolism, and energy production and conversion in the La-EBPR system increased significantly following the addition of LZGA (Fig. 5f).

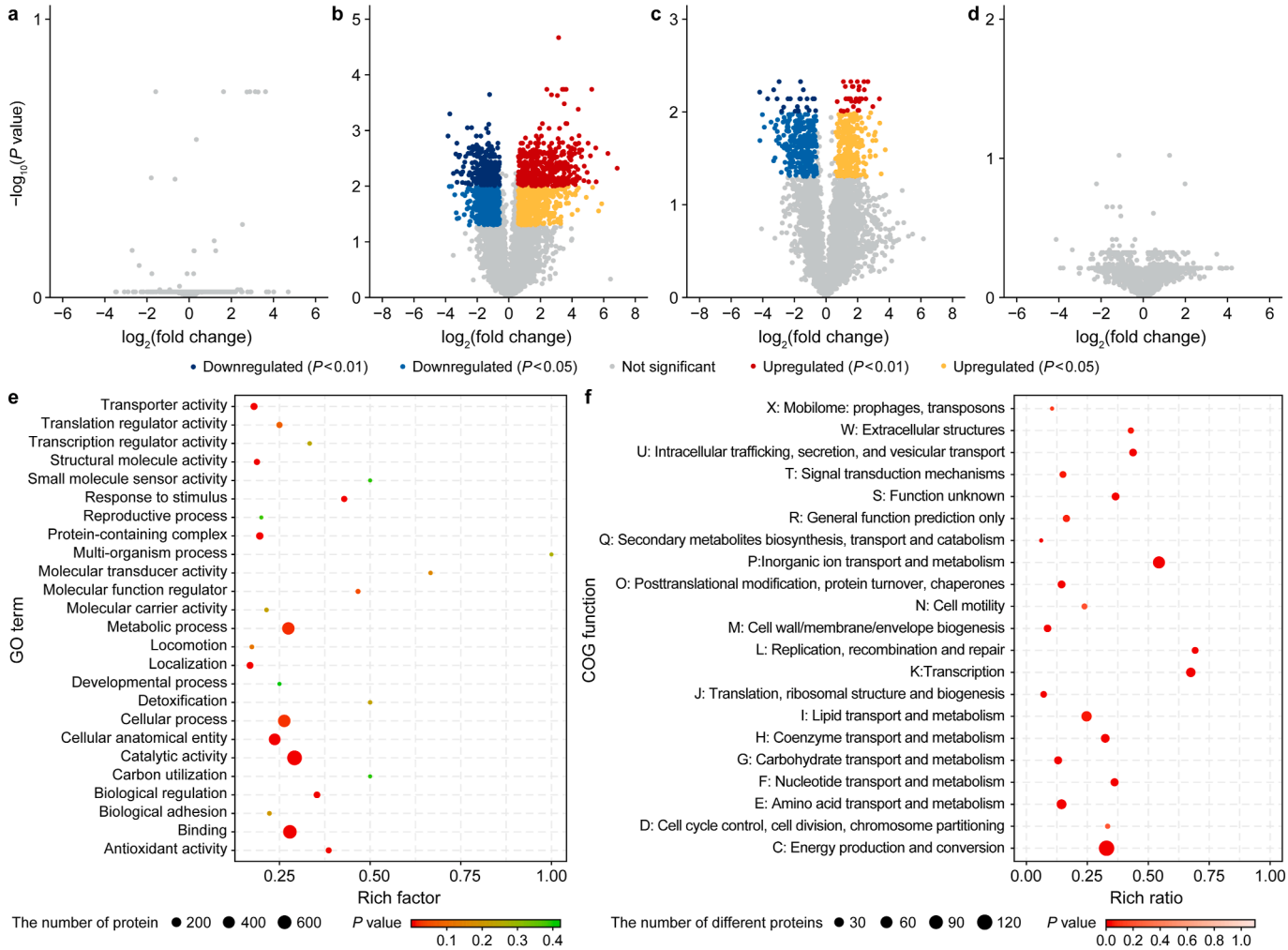

Fig. 5. Temporal changes in protein abundance between the traditional enhanced biological phosphorus removal (EBPR) and La-EBPR systems. a–d, Volcano plots showing differential protein expression levels between the traditional EBPR and La-EBPR systems amended with 15 mg L^{-1} La-containing aerogel during the initial phase (**a**), after 20 days (**b**), 40 days (**c**), and 60 days (**d**) of operation. **e**, Gene Ontology (GO) classification of differentially expressed proteins. **f**, Classification of orthologous groups (COG) of differentially expressed proteins.

To better understand the functions of LZGA on proteins related to PAOs in the La-EBPR system, we identified a protein pathway regulatory network involving 4200 proteins and their associated pathways. In the La-EBPR system, the addition of LZGA upregulated multiple proteins and pathways related to PAOs (Fig. 6). A large number of proteins directly associated with the metabolic transformations, characteristic of EBPR, were upregulated (the protein accessions and accession descriptions are provided in Supplementary Table S2). Furthermore, we hypothesized that if LZGA played important roles in the La-EBPR system, the proteins correlated with LZGA would be enriched in pathways associated with P removal. After the introduction of LZGA beads, the enzymes associated with the glyoxylate/tricarboxylic acid (TCA) cycle exhibited the most significant increase in the La-EBPR system. The TCA cycle is a crucial component of EBPR. During the aerobic stage, the TCA cycle generates substantial amounts of adenosine triphosphate (ATP), providing energy for PAOs to capture P from the environment and synthesize polyphosphate, thereby facilitating efficient P removal from wastewater [65]. Our proteomic analysis identified an increase in succinate dehydrogenase/fumarate reductase iron-sulfur subunit (SuccDH) of *Candidatus* Accumulibacter. As part of the TCA cycle, the increase in SuccDH enhanced the rates of acetic acid absorption and polyhydroxyalkanoate production, thereby promoting P uptake by PAOs. Three other enzymes linked to the TCA cycle were highly expressed, including pyruvate dehydrogenase, which connects the TCA cycle and subsequent oxidative phosphorylation to glycolysis, gluconeogenesis, and lipid and amino acid metabolism pathways [66]. Considering these results, the appropriate LZGA concentration can enhance TCA cycle activity in the La-EBPR system. Several proteins involved in oxidative phosphorylation, which is related to ATP production in the La-EBPR system, were also highly expressed. The expression of polyphosphate kinase 1 (PPK1) in *Dechloromonas* was significantly increased in the La-EBPR system. PPK1 is the principal enzyme responsible for the reversible synthesis of polyphosphate (poly P) from the terminal PO_4^{3-} of ATP [67]. The process of P accumulation in microorganisms under aerobic or anoxic conditions is mainly catalyzed by PPK1. The release of active La components in LZGA promoted PPK1 production and directly enhanced P release and uptake in the La-EBPR system. The energy

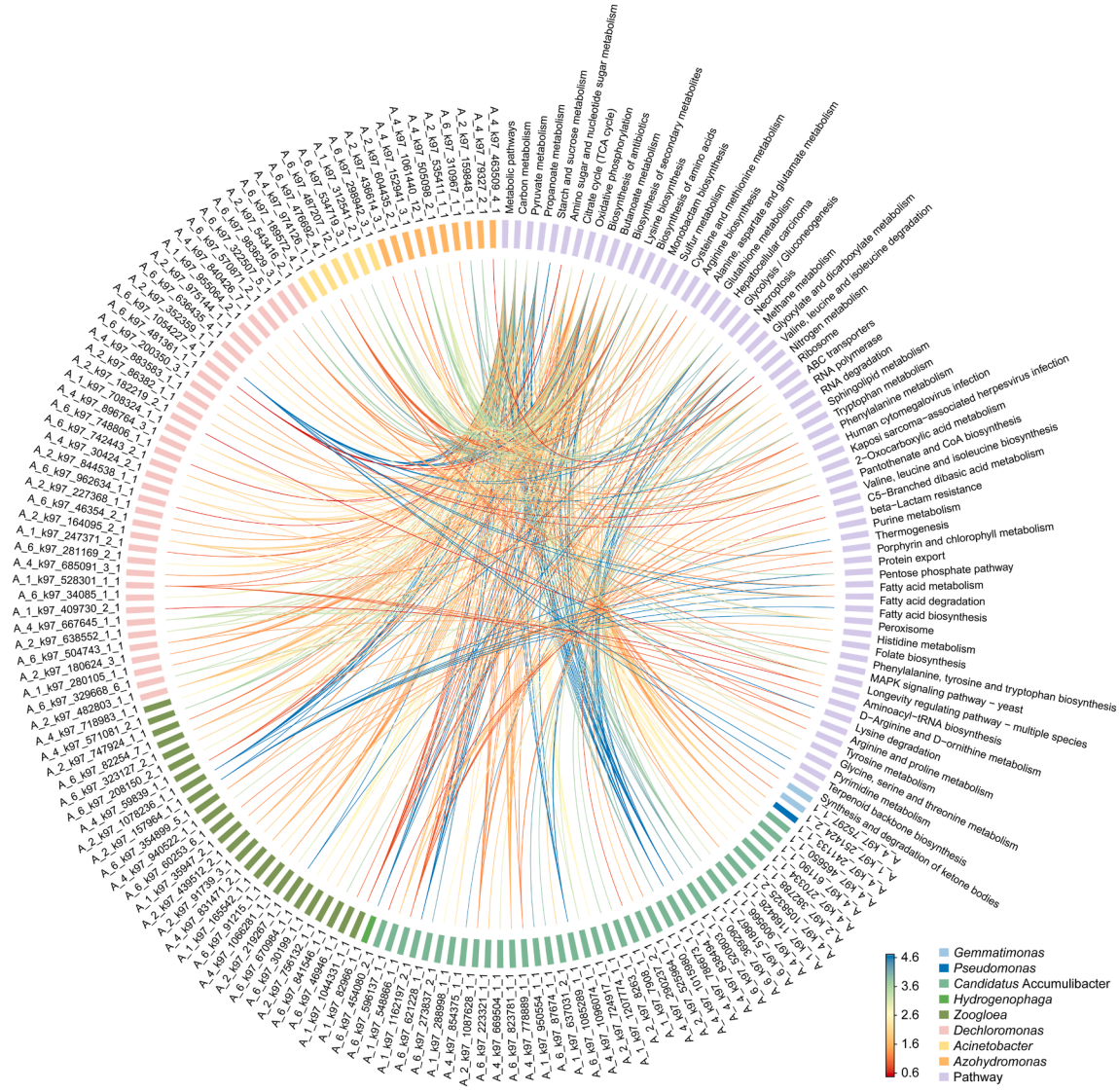

Fig. 6. Protein–pathway regulatory network in the lanthanum-enhanced biological phosphorus removal (La-EBPR) system. Protein–pathway network linking phosphorus-accumulating organism (PAO)-related genera, proteins, and enriched metabolic pathways in the La-EBPR system.

metabolism of many microorganisms is based on glycolysis. In the aerobic phase, glycolysis is a minor source of energy, with approximately 95% of ATP production coming from the TCA cycle and oxidative phosphorylation. In contrast, the PAOs in the anaerobic stage rely almost exclusively on glycolysis for ATP production, and therefore, the enzymes related to glycolysis should not be ignored [68]. When examining specific changes in proteins involved in glycogen degradation and synthesis, we observed significant increases in phosphoglycerate kinase, type I glyceraldehyde-3-phosphate dehydrogenase, glucose-6-phosphate isomerase, and several other proteins related to pyruvate metabolism. In addition to changes in energy metabolism, the expression of proteins involved in PHA synthesis and the PO_4^{3-} transport system increased following the addition of LZGA. PHA plays a crucial role in the metabolism and growth of PAOs, thereby impacting the efficiency of the EBPR system [69]. The proteomic results indicated a significant increase in acetyl-CoA acetyltransferase, which can supply the reducing equivalents required for PHA synthesis during the anaerobic phase. Furthermore, four different ATP-binding cassette (ABC) transporters associated with the ABC-type phosphate-specific transport system (Pst) showed a tendency to increase. In PAOs, the Pst transport system couples ATP hydrolysis to the translocation of PO_4^{3-} across the inner membrane, allowing PAOs to actively transport and use PO_4^{3-}. The increased expression of PHA synthesis and the phosphate transport system can have direct implications for the biochemical and bioenergetic characterization of the PO_4^{3-} transport systems of PAOs in the context of EBPR.

Based on the experimental conclusions and the mechanism analysis outlined above, we propose a P transformation and transportation model for the La-EBPR system (Fig. 7). When LZGA was introduced into the reactors, the La-EBPR system was established. The release of active La components from LZGA accelerated K^+ channel opening and effectively enhanced the synchronized metabolism of K^+ and P. Some of the active La components bound to *Zoogloea*, promoting the formation of EPS. Additionally, LZGA facilitated the capture of P by EPS, resulting in P enrichment. When the PAOs enveloped by EPS sensed an increase in P concentration, their P metabolic capacity increased. Previous studies have demonstrated that the three-dimensional network structure of bacterial cell walls can provide accessible binding sites for La [70]. Another portion of the active La components formed complexes with PAOs and DPAOs, significantly enhancing the growth of enzymes related to the TCA cycle, oxidative phosphorylation, and other energy metabolic processes, as well as reinforcing the phosphate transport system. Furthermore, the abundance of PAOs increased, accompanied by a marked upregulation of PAO-associated proteins, including those from *Candidatus* Accumulibacter, thereby enhancing phosphorus removal in the La-EBPR system. Moreover, La can bind to the floc surface to neutralize the negative charge on the sludge surface, thereby improving sludge sedimentation performance. Consequently, in the La-EBPR system, LZGA plays a crucial role in the functioning of PAOs and EPS.

4. Conclusions

In this study, we demonstrated a leverage strategy to enhance P removal in the La-EBPR system by boosting PAO activity. Following the addition of 15 mg L^{-1} LZGA to the La-EBPR system, the TP concentration decreased significantly to 0.14 mg L^{-1}. Compared with traditional chemical P removal methods, the proposed La-EBPR system offers a remarkable reduction in chemical consumption of approximately two orders of magnitude. Furthermore, LZGA increased EPS production, enhanced P uptake, and improved sludge sedimentation performance. The release of active La components from LZGA improved K^+ channel function at the cell membrane, thereby enhancing the synchronized metabolism of K^+ and P. Additionally, LZGA can selectively modulate microorganisms within the La-EBPR system. High-throughput

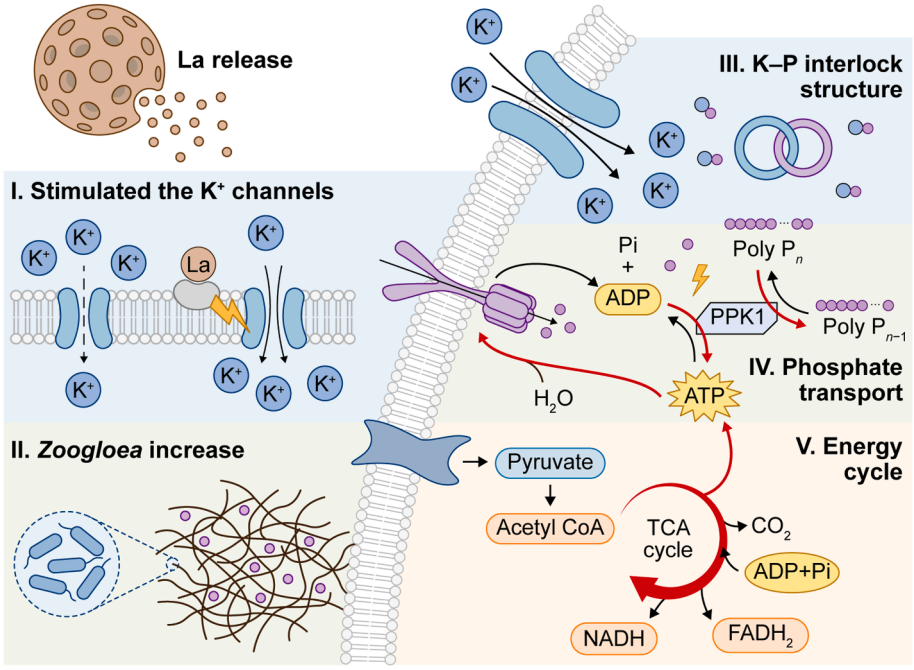

Fig. 7. Proposed mechanism of phosphorus transformation and transport in the lanthanum-enhanced biological phosphorus removal (La-EBPR) system. Schematic model illustrating how La-containing aerogel promotes phosphorus transformation and transport in the La-EBPR system, including effects on phosphorus-accumulating organism activity, extracellular polymeric substances-associated phosphorus, K^+ channel activation, phosphate transport, and cellular energy metabolism. PPK1, polyphosphate kinase1; ADP, adenosine diphosphate; ATP, adenosine triphosphate; TCA cycle, tricarboxylic acid cycle; NADH, nicotinamide adenine dinucleotide; $FADH_2$, flavine adenine dinucleotide, reduced.

sequencing results revealed that the optimal concentration of LZGA favored PAO growth. Our study provides evidence of higher expression levels of proteins involved in energy metabolism and the PO_4^{3-} transport system, directly highlighting for the first time the significance of La in EBPR metabolism. This study is expected to serve as a valuable reference for the development of EBPR strategies with La as a central component.

CRediT authorship contribution statement

Bohan Liu: Writing – review & editing, Writing – original draft, Formal analysis, Conceptualization. **Jun Nan:** Supervision, Funding acquisition. **Rongcheng He:** Investigation. **Haiyang Wei:** Investigation. **Tianyi Zhao:** Methodology. **Yibo Zhang:** Investigation. **Ruixue Jiang:** Data curation. **Fangmin Wu:** Conceptualization. **Zhencheng Ge:** Validation. **Xuesong Ye:** Visualization. **Wei Wang:** Writing – review & editing. **Jun Ma:** Visualization.

Declaration of competing interest

The authors declare that they have no known competing financial interests or personal relationships that could have appeared to influence the work reported in this paper.

Acknowledgements

The research was supported by the National Natural Science Foundation of China (No. 52400024); China National Postdoctoral Program for Innovative Talents (BX20230480); Open Project of State Key Laboratory of Urban-rural Water Resource & Environment, Harbin Institute of Technology (No.QA202431), and the National Key R&D Program of China (Grant No. 2022YFC3203402).

Appendix A. Supplementary data

Supplementary data to this article can be found online at https://doi.org/10.1016/j.ese.2026.100708.

References

[1] L. Yang, S. Zheng, S. Michel, D. Renata, J. Cees, Electrochemical recovery of phosphorus from wastewater using tubular stainless-steel cathode for a scalable long-term operation, Water Res. 199 (2021) 117199.
[2] B. Wu, I.M.C. Lo, Surface functional group engineering of CeO_2 particles for enhanced phosphate adsorption, Environ. Sci. Technol. 54 (7) (2020) 4601–4608.
[3] J. Yu, C. Xiang, G. Zhang, H. Wang, Q. Ji, J. Qu, Activation of lattice oxygen in LaFe (Oxy)hydroxides for efficient phosphorus removal, Environ. Sci. Technol. 53 (2019) 9073–9080.
[4] R.J. Diaz, R. Rosenberg, Spreading dead zones and consequences for marine ecosystems, Science 321 (5891) (2008) 926–929.
[5] D.J. Conley, H.W. Paerl, R.W. Howarth, D.F. Boesch, S.P. Seitzinger, K.E. Havens, C. Lancelot, G.E. Likens, Ecology controlling eutrophication: Nitrogen and phosphorus, Science 323 (5917) (2009) 1014–1015.
[6] X. Wang, G. Daigger, W. de Vries, C. Kroeze, M. Yang, N.Q. Ren, J.X. Liu, D. Butler, Impact hotspots of reduced nutrient discharge shift across the globe with population and dietary changes, Nat. Commun. 10 (2019) 2627.
[7] P. Zhang, M.M. He, Z.K. Xu, F.K. Li, D.Z. Fang, C. Li, C.C. Lv, X.P. Mo, K.X. Li, H. Wang, Incorporation of edge-N into La-doped hierarchical carbon framework enables high-efficiency phosphate electrosorption: boosting accessible active centers and bridging charge transfer paths, Chem. Eng. J. 481 (2024) 148518.
[8] Y.Y. Peng, S.B. He, F. Wu, Biochemical processes mediated by iron-based materials in water treatment: enhancing nitrogen and phosphorus removal in low C/N ratio wastewater, Sci. Total Environ. 775 (2021) 145137.
[9] L.W. Wu, D.L. Ning, B. Zhang, Y. Li, P. Zhang, X.Y. Shan, Q.T. Zhang, M.R. Brown, Z.X. Li, J.D. Van Nostrand, F.Q. Ling, N.J. Xiao, Y. Zhang, J. Vierheilig, G.F. Wells, Y.F. Yang, Y. Deng, Q.C. Tu, A.J. Wang, T. Zhang, Z.L. He, J. Keller, P.H. Nielsen, P.J.J. Alvarez, C.S. Criddle, M. Wagner, J.M. Tiedje, Q. He, T.P. Curtis, D.A. Stahl, L. Alvarez-Cohen, B.E. Rittmann, X.H. Wen, J.Z. Zhou, Global diversity and biogeography of bacterial communities in wastewater treatment plants, Nat. Microbiol. 4 (7) (2019) 1183–1195.
[10] M.S. Dueholm, M. Nierychlo, K.S. Andersen, V. Rudkjobing, S. Knutsson, M. Albertsen, P.H. Nielsen, MiDAS 4: a global catalogue of full-length 16S rRNA gene sequences and taxonomy for studies of bacterial communities in wastewater treatment plants, Nat. Commun. 13 (1) (2022) 1908.
[11] J.W. Zhao, Q.J. Yuan, Y.J. Sun, J. Zhang, D.L. Zhang, R.X. Bian, Effect of fluoxetine on enhanced biological phosphorus removal using a sequencing batch reactor, Bioresour. Technol. 320 (2021) 124396.
[12] Q.P. Dan, Q. Zhang, T. Wang, H.B. Wang, Y.Z. Peng, Floc management enables integrated anammox and enhanced biological phosphorus removal for sustainable ultra-efficient nutrient removal, Nat. Water 3 (2) (2025) 201–210.
[13] H.M. Huang, J.H. Liu, P. Zhang, D.D. Zhang, F.M. Gao, Investigation on the simultaneous removal of fluoride, ammonia nitrogen and phosphate from semiconductor wastewater using chemical precipitation, Chem. Eng. J. 307 (2017) 696–706.
[14] B.L. Wu, J. Wan, Y.Y. Zhang, B.C. Pan, I.M.C. Lo, Selective phosphate removal from water and wastewater using sorption: process fundamentals and removal mechanisms, Environ. Sci. Technol. 54 (2020) 50–66.
[15] S. Liu, J. Liu, Y. Zhou, C.Z. Liao, Z.K. Ni, S.R. Wang, Simultaneous removal of dissolved inorganic and organic phosphorus by magnetic α-Fe_2O_3/LaOCl composites: performance, mechanisms and applicability, Sep. Purif. Technol. 348 (2024) 127814.
[16] C. Cepan, A.E. Segneanu, O. Grad, M. Mihailescu, M. Cepan, I. Grozescu, Assessment of the different type of materials used for removing phosphorus from wastewater, Materials 14 (2021) 4371.
[17] U.A. Toor, H. Shin, D.J. Kim, Mechanistic insights into nature of complexation between aluminum and phosphates in polyaluminum chloride treated sludge for sustainable phosphorus recovery, J. Ind. Eng. Chem. 71 (2019) 425–434.
[18] C. Auger, S.W. Han, V.P. Appanna, S.C. Thomas, G. Ulibarri, V.D. Appanna, Metabolic reengineering invoked by microbial systems to decontaminate aluminum: implications for bioremediation technologies, Biotechnol. Adv. 31 (2) (2013) 266–273.
[19] B.G. Wang, W. Zeng, Z.W. Fan, C.Y. Wang, Q.G. Meng, Y.Z. Peng, Effects of polyaluminium chloride addition on community structures of polyphosphate and glycogen accumulating organisms in biological phosphorus removal (BPR) systems, Bioresour. Technol. 297 (2020) 122431.
[20] W.J. Xia, H. Wang, L.Q. Yu, G.F. Li, J.R. Xiong, X.Y. Zhu, X.C. Wang, J.R. Zhang, B.C. Huang, R.C. Jin, Coagulants put phosphate-accumulating organisms at a competitive disadvantage with glycogen-accumulating organisms in enhanced biological phosphorus removal system, Bioresour. Technol. 346 (2022) 126658.
[21] J. Li, S. Tabassum, Minimizing excess sludge production under synergistic effect of diatomite and uncoupling agent 2,4-dinitrophenol: an in-depth study, Clean. Eng. Technol. 6 (2022) 100353.
[22] L.F. Tang, M.M. Gao, S. Liang, S.G. Wang, X.H. Wang, Enhanced biological phosphorus removal sustained by aeration-free filamentous microalgal-bacterial granular sludge, Water Res. 253 (2024) 121315.
[23] H. Wang, Y.B. Wang, G.Q. Zhang, Z. Zhao, F. Ju, Temporal dynamics and performance association of the tetrasphaera-enriched microbiome for enhanced biological phosphorus removal, Engineering 29 (2023) 168–178.
[24] Z.J. Zhang, H. Li, J. Zhu, W.P. Liu, X. Xu, Improvement strategy on enhanced biological phosphorus removal for municipal wastewater treatment plants: full-scale operating parameters, sludge activities, and microbial features, Bioresour. Technol. 102 (7) (2011) 4646–4653.
[25] H.L. Zhang, W. Fang, Y.P. Wang, G.P. Sheng, C.W. Xia, R.J. Zeng, H.Q. Yu, Species of phosphorus in the extracellular polymeric substances of EBPR sludge, Bioresour. Technol. 142 (2013) 714–718.
[26] R. Barat, T. Montoya, A. Seco, The role of potassium, magnesium and calcium in the enhanced biological phosphorus removal treatment plants, Environ. Technol. 26 (9) (2005) 983–992.
[27] D. Aguado, T. Montoya, J. Ferrer, A. Seco, Relating ions concentration variations to conductivity variations in a sequencing batch reactor operated for enhanced biological phosphorus removal, Environ. Modell. Softw. 21 (6) (2006) 845–851.
[28] J. Tytgat, P. Daenens, Effect of lanthanum on voltage-dependent gating of a cloned Mammalian neuronal potassium channel, Brain Res. 749 (2) (1997) 232–237.
[29] C.S. Watkins, A. Mathie, Modulation of the gating of the transient outward potassium current of rat isolated cerebellar granule neurons by lanthanum, Pflilg. Arch. 428 (3–4) (1994) 209–216.
[30] X.M. Li, J.Z. Ni, J.W. Chen, F. Hwang, Effects of La^{3+} on lipid fluidity land structural transitions in human erythrocyte membranes, Biochem. Mol. Biol. Int. 45 (2) (1998) 323–330.
[31] Q.X. Liu, Z.Q. Jiang, M.Y. Qiu, M.E. Andersen, M.J.C. Crabbe, X. Wang, Y.X. Zheng, W.D. Qu, Subchronic exposure to low-level lanthanum, cerium, and yttrium mixtures altered cell cycle and increased oxidative stress pathways in human LO-2 hepatocytes but did not cause malignant transformation, Environ. Sci. Technol. 58 (50) (2024) 22002–22013.
[32] H. Zhao, W.D. Hao, H.E. Xu, L.Q. Shang, Y.Y. Lu, Gene expression profiles of hepatocytes treated with $La(NO_3)_3$ of rare earth in rats, World J. Gastroenterol. 10 (11) (2004) 1625–1629.
[33] A.M. Panichev, Rare earth elements: review of medical and biological properties and their abundance in the rock materials and mineralized spring waters in the context of animal and human geophagia reasons evaluation, Achieve, Life Sci. 9 (2) (2015) 95–103.

[34] M. Richter-Laskowska, P. Trybek, D.V. Delfino, A. Wawrzkiewicz-Jalowiecka, Flavonoids as modulators of potassium channels, Int. J. Mol. Sci. 24 (2) (2023) 1311.
[35] D.A. Doyle, J.M. Cabral, R.A. Pfuetzner, A.L. Kuo, J.M. Gulbis, S.L. Cohen, B.T. Chait, R. MacKinnon, The structure of the potassium channel: molecular basis of K^+ conduction and selectivity, Science 280 (5360) (1998) 69–77.
[36] APHA, Standard Methods for the Examination of Water and Wastewater, 21sted, American Public Health Association, Washington, DC, 2005.
[37] Q.L. He, W. Zhang, S.L. Zhang, H.Y. Wang, Enhanced nitrogen removal in an aerobic granular sequencing batch reactor performing simultaneous nitrification, endogenous denitrification and phosphorus removal with low superficial gas velocity, Chem. Eng. J. 326 (2017) 1223–1231.
[38] B. FrØlund, T. Griebe, P.H. Nielsen, Enzymatic activity in the activated-sludge floc matrix, Appl. Microbiol. Biotechnol. 43 (1995) 755–761.
[39] P. Gerhardt, W.A. Wood, N.R. Krieg, R. Murray, Methods for General and Molecular Bacteriology, ASM Press. Methods for General & Molecular Microbiology, 1994.
[40] F. Gao, J. Nan, S.N. Li, Y.R. Wang, Modeling and simulation of a biological process for treating different COD: n ratio wastewater using an extended ASM1 model, Chem. Eng. J. 332 (2017) 671–681.
[41] Y. Shi, X. Wang, A. Huang, Proteomic analysis and food-grade enzymes of Moringa oleifer Lam. a Lam. Flower, Int. J. Biol. Macromol. 115 (2018) 883–890.
[42] D.K. Pyne, S. Chatterjee, S. Pramanik, A. Halder, Temperature-induced photoluminescence amplification of graphene oxide-polyaniline composite through interaction modulated charge transfer, Mater. Chem. Phys. 318 (2024) 129241.
[43] J.C. Tu, Y.P. Zhang, L.L. Chen, X. Chen, Y.P. Li, X.H. Min, Q. Chen, T. Chen, K.L. Wang, Y.Q. Luo, Optimization of $FeSO_4$-$Al_2(SO_4)_3$ composite flocculant for enhanced phosphorus removal in wastewater treatment: a response surface methodology study, Processes 13 (3) (2025) 882.
[44] Y.T. Hameed, A. Idris, S.A. Hussain, N. Abdullah, A tannin-based agent for coagulation and flocculation of municipal wastewater: chemical composition, performance assessment compared to polyaluminum chloride, and application in a pilot plant, J. Environ. Manag. 184 (2016) 494–503.
[45] J. Fan, H. Zhang, J.S. Ye, B. Ji, Chemical stress from Fe salts dosing on biological phosphorus and potassium behavior, Water Sci. Technol. 77 (5–6) (2018) 1222–1229.
[46] M. Robb, B. Greenop, Z. Goss, G. Douglas, J. Adeney, Application of phoslock (TM), an innovative phosphorus binding clay, to two Western Australian waterways: preliminary findings, Hydrobiologia 494 (2003) 237–243.
[47] X.T. Zhang, F.L. Sun, J.J. He, H.B. Xu, F.Y. Cui, W. Wang, Robust phosphate capture over inorganic adsorbents derived from lanthanum metal organic frameworks, Chem. Eng. J. 326 (2017) 1086–1094.
[48] L.P. Fang, R. Liu, J. Li, C.H. Xu, L.Z. Huang, D.S. Wang, Magnetite/lanthanum hydroxide for phosphate sequestration and recovery from lake and the attenuation effects of sediment particles, Water Res. 130 (2018) 243–254.
[49] G.P. Sheng, H.Q. Yu, X.Y. Li, Extracellular polymeric substances (EPS) of microbial aggregates in biological wastewater treatment systems: a review, Biotechnol. Adv. 28 (6) (2010) 882–894.
[50] A. Melo, J. Costa, C. Quintelas, E.C. Ferreira, D.P. Mesquita, Effect of ibuprofen on extracellular polymeric substances (EPS) production and composition, and assessment of microbial structure by quantitative image analysis, J. Environ. Manag. 293 (2021) 112852.
[51] L.L. Xing, J.X. Yang, B.J. Ni, C. Yang, C.Y. Yuan, A. Li, Insight into the generation and consumption mechanism of tightly bound and loosely bound extracellular polymeric substances by mathematical modeling, Sci. Total Environ. 811 (2022) 152359.
[52] T.T. More, J.S.S. Yadav, S. Yan, R.D. Tyagi, R.Y. Surampalli, Extracellular polymeric substances of bacteria and their potential environmental applications, J. Environ. Manag. 144 (2014) 1–25.
[53] W.W. Li, H.Q. Yu, Insight into the roles of microbial extracellular polymer substances in metal biosorption, Bioresour. Technol. 160 (2014) 15–23.
[54] H.X. Shi, J. Wang, S.Y. Liu, J.S. Guo, F. Fang, Y.P. Chen, P. Yan, New insight into filamentous sludge bulking: potential role of AHL-mediated quorum sensing in deteriorating sludge floc stability and structure, Water Res. 212 (2022) 118096.
[55] L. Zhu, M.L. Lv, X. Dai, Y.W. Yu, H.Y. Qi, X.Y. Xu, Role and significance of extracellular polymeric substances on the property of aerobic granule, Bioresour. Technol. 107 (2012) 46–54.
[56] J.Y. Ye, H. Gao, J.K. Wu, R. Yu, Effects of ZnO nanoparticles on flocculation and sedimentation of activated sludge in wastewater treatment process, Environ. Res. 192 (2021) 110256.
[57] Y. Wen, W.L. Zheng, Y.D. Yang, A.S. Cao, Q. Zhou, Influence of Al^{3+} addition on the flocculation and sedimentation of activated sludge: comparison of single and multiple dosing patterns, Water Res. 75 (2015) 201–209.
[58] T.E. Cloete, D.J. Oosthuizen, The role of extracellular exopolymers in the removal of phosphorus from activated sludge, Water Res. 35 (2001) 3595–3598.
[59] W.W. Li, H.L. Zhang, G.P. Sheng, H.Q. Yu, Roles of extracellular polymeric substances in enhanced biological phosphorus removal process, Water Res. 86 (2015) 85–95.
[60] S.S. Yang, J.W. Pang, W.Q. Guo, X.Y. Yang, Z.Y. Wu, N.Q. Ren, Z.Q. Zhao, Biological phosphorus removal in an extended ASM2 model: roles of extracellular polymeric substances and kinetic modeling, Bioresour. Technol. 232 (2017) 412–416.
[61] L.L. Blackall, G. Crocetti, A.M. Saunders, P.L. Bond, A review and update of the microbiology of enhanced biological phosphorus removal in wastewater treatment plants, Anton. Leeuw. Int. J. G. 81 (2002) 681–691.
[62] C.S. Zhou, J.W. Wu, B.F. Liu, W.L. Ma, S.S. Yang, G.L. Cao, (Micro) nanoplastics promote the risk of antibiotic resistance gene propagation in biological phosphorus removal system, J. Hazard. Mater. 431 (2022) 128547.
[63] S.M. Zhao, W. Xu, W.L. Zhang, H. Wu, C. Guang, W.M. Mu, In-depth biochemical identification of a novel methyl parathion hydrolase from Azohydromonas australica and its high effectiveness in the degradation of various organophosphorus pesticides, Bioresour. Technol. 323 (2021) 124641.
[64] W.X. An, F. Guo, Y.L. Song, N. Gao, S.J. Bai, J.C. Dai, H.H. Wei, L.P. Zhang, D.Z. Yu, M. Xia, Y. Yu, M. Qi, C.Y. Tian, H.F. Chen, Z.B. Wu, T. Zhang, D.R. Qiu, Comparative genomics analyses on EPS biosynthesis genes required for floc formation of Zoogloea resiniphila and other activated sludge bacteria, Water Res. 102 (2016) 494–504.
[65] N. Majed, T. Chernenko, M. Diem, A.Z. Gu, Identification of functionally relevant populations in enhanced biological phosphorus removal processes based on intracellular polymers profiles and insights into the metabolic diversity and heterogeneity, Environ. Sci. Technol. 46 (9) (2012) 5010–5017.
[66] P.C. Lemos, L.S. Serafim, M.M. Santos, M.A.M. Reis, H. Santos, Metabolic pathway for propionate utilization by phosphorus-accumulating organisms in activated sludge: C-13 labeling and in vivo nuclear magnetic resonance, Appl. Environ. Microbiol. 69 (1) (2003) 241–251.
[67] M. Liang, S. Frank, H. Luensdorf, M.J. Warren, M.B. Prentice, Bacterial microcompartment-directed polyphosphate kinase promotes stable polyphosphate accumulation in E. coli, J. Biotechnol. 12 (3) (2017) 1600415.
[68] A.B. Lanham, A. Oehmen, A.M. Saunders, G. Carvalho, P.H. Nielsen, M.A.M. Reis, Metabolic versatility in full-scale wastewater treatment plants performing enhanced biological phosphorus removal, Water Res. 47 (19) (2013) 7032–7041.
[69] R.Y. Wang, Y.M. Li, W.L. Chen, J.T. Zou, Y.G. Chen, Phosphate release involving PAOs activity during anaerobic fermentation of ESPR sludge and the extension of ADM1, Chem. Eng. J. 287 (2016) 436–447.
[70] A.C. Texier, Y. Andrès, M. Illemassene, C.P. Le, Characterization of lanthanide ions binding sites in the cell wall of Pseudomonas aeruginosa, Environ. Sci. Technol. 34 (4) (2000) 610–615.